Available online at www.sciencedirect.com
SCIENCE DIRECT®
Journal of Solid State Chemistry 174 (2003) 189–197
JOURNAL OF SOLID STATE CHEMISTRY
http://elsevier.com/locate/jssc

Crystallographic investigation of the Co–B–O system

J.L.C. Rowsell,[1] N.J. Taylor, and L.F. Nazar*

Department of Chemistry, University of Waterloo, 200 University Avenue West, Waterloo, Ont., Canada N2L 3G1

Received 27 October 2002; received in revised form 27 January 2003; accepted 14 April 2003

Abstract

The crystalline phases within the Co–B–O system have been investigated with a combination of powder and single crystal X-ray diffraction. By varying the synthetic conditions, four pure phases can be made by solid-state reaction: $Co_3(BO_3)O_2$, a homometallic ludwigite; $Co_3(BO_3)_2$, an orthoborate with the kotoite structure; $Co_2(B_2O_5)$, a pyroborate; and the tetraborate $Co(B_4O_7)$. Herein, we report the first structural refinement of the latter phase (orthorhombic, space group *Pbca*, $a = 8.1189(7)$ Å, $b = 8.621(1)$ Å, $c = 13.737(1)$ Å, $V = 961.5(2)$ Å^3, $Z = 8$, $R_1 = 0.0319$, w$R_2 = 0.0693$ [$I > 2\sigma(I)$]). The pyroborate structure was also refined by single crystal methods in order to match the calculated powder diffraction pattern with the observed pattern (triclinic, space group $P\bar{1}$, $a = 3.1689(3)$ Å, $b = 6.1530(5)$ Å, $c = 9.2734(7)$ Å, $\alpha = 104.253(4)^\circ$, $\beta = 90.821(4)^\circ$, $\gamma = 92.098(5)^\circ$, $V = 175.08(3)$ Å^3, $Z = 2$, $R_1 = 0.0159$, w$R_2 = 0.0366$ [$I > 2\sigma(I)$]). Flux growth of $Co(B_4O_7)$ also yielded single crystals of the new compound $Co_4(BO_2)_6O$ (cubic, space group $I\bar{4}3m$, $a = 7.4825(3)$ Å, $V = 418.93(3)$ Å^3, $Z = 2$, $R_1 = 0.0176$, w$R_2 = 0.0373$ [$I > 2\sigma(I)$]).

Keywords: Metal borates; Cobalt; Single crystal X-ray diffraction; Magnetic frustration

1. Introduction

Borate compounds have been the subjects of crystallographic study for much of the last century, primarily due to the myriad of structure types attainable by boron's trigonal or tetrahedral coordination. Current research is focused mainly on anhydrous main group metal borates for non-linear optical applications, where the presence of transition metals is avoided to maintain ultraviolet transparency [1]. Transition metal borates, however, display such important properties as catalytic activity [2], unique magnetic behavior [3,4], and reversible Li-ion uptake [5,6]. We have undertaken a thorough investigation of the Co–B–O system to uncover potentially interesting phases, using solid-state syntheses and flux methods for crystal growth. This study has already yielded the $Na_2Co_2B_{12}O_{21}$ framework, which consists of a novel metaborate tunnel structure housing exchangeable sodium ions [7].

The published CoO–B_2O_3 phase diagram [8] only exhibits two defined ternary compounds; the orthoborate $Co_3(BO_3)_2$ and the pyroborate $Co_2(B_2O_5)$. By measuring the composition dependence of the CoO chemical potential in CoO–B_2O_3 mixtures, Hauck and Muller confirmed the stoichiometries of these stable phases and identified a third: $Co(B_4O_7)$, reported to be isostructural with $Mg(B_4O_7)$ [9]. The crystal structures of the first two compounds were originally elucidated by Berger, and were the first examples of their respective types [10,11]. Not until several years later was another compound detected, $Co_3(BO_3)O_2$, a homometallic ludwigite [12]. Both the orthoborate and ludwigite structures have been refined in recent years [13,14] and single crystals of all but $Co(B_4O_7)$ can be grown directly from the melt.

Binary transition metal borates (or ternary *M*–B–O compounds) certainly exhibit greater structural diversity than those few types listed above. While there is powder X-ray diffraction (XRD) data for dozens of phases, less than 20 structure types have been well established. There is a trend across the first period, as elements switch from preferring the trivalent to the divalent oxidation state. The elements early in the period exhibit the calcite structure $M^{III}(BO_3)$ (M = Sc [15], Ti [16], V [17], Cr [18], Fe [19]), while Cr and Fe also display the norbergite structure $M_3^{III}(BO_4)O_2$ [6,20]. Manganese, iron and

*Corresponding author. Fax: 001-519-746-0435.
E-mail address: lfnazar@uwaterloo.ca (L.F. Nazar).
[1] Present address: University of Michigan, Ann Arbor, MI, USA.

0022-4596/03/$ - see front matter © 2003 Elsevier Science (USA). All rights reserved.
doi:10.1016/S0022-4596(03)00217-2

cobalt can exist in mixed oxidation states in the ludwigite $M^{III}M_2^{II}(BO_3)O_2$ (M = Mn [21], Fe [22] Co [14]) and warwickite $M^{III}M^{II}(BO_3)O$ (M = Mn [23], Fe [3]) phases. Curiously, Mn forms no trivalent borates; evidence for $MnBO_3$ based on powder diffraction studies [24] can probably be attributed to the presence of $Mn_2(BO_3)O$. Elements later in the periodic table produce structures including $M^{II}(B_4O_7)$ (M = Mn [25], Zn [26], Cd [27], Hg [28]), $M_4^{II}(BO_2)_6O$ (M = Zn [29], Hg [30]), and $M^{II}(BO_2)_2$ (M = Cu [31], Pd [32]). Compounds with nominal composition $M_3^{II}B_2O_6$ exist, although their structures differ between Cu [33], Zn [34], Hg [35] and the kotoite form (M = Mn [36]), Co [13], Ni [13], Cd [37]). Zinc forms the unique phase $Zn_4(BO_3)_2O$ [38] under hydrothermal conditions, while cadmium is the only transition element other than cobalt shown to form a pyroborate $M^{II}(B_2O_5)$ [39]. Other known second and third transition series anhydrous borates include those of silver(I) ($AgBO_2$ [40], $Ag_2B_8O_{13}$ [41], and two forms of $Ag_3(BO_3)$ [42,43]) and those with the zircon structure $M^{V}(BO_4)$ (M = Nb [44], Ta [45]).

In the structures listed above, the borate building unit has been enclosed in parentheses to denote its geometry. Thus, frameworks such as calcite, ludwigite, warwickite, and kotoite only contain isolated borate triangles, while the norbergite and zircon structures possess discrete borate tetrahedra. Since the connectivity of polyborates is not at all denoted by their formulae (i.e., $AgBO_2$), schemes have been proposed to better describe and classify such structures [46].

2. Experimental

2.1. Synthesis

Numerous starting materials were employed for the solid-state syntheses, including $Co(NO_3)_2 \cdot 6H_2O$, Co(acac)$_3$, $CoCO_3 \cdot xH_2O$, Co_3O_4 (all from Aldrich), CoO and B_2O_3 (Alfa Aesar), $CoSO_4 \cdot 7H_2O$ and H_3BO_3 (Baker). Materials were ground in a sialon mortar mounted on a planetary ball mill (Fritsch) for two 15 min periods at moderate speed. Samples were checked for homogeneity and adhesion to the sides of the mortar between grinding periods. After preparing mixtures varying in Co:B stoichiometry from 5:1 to 1:10, pellets were formed under 10 tons of pressure in a 13 mm diameter KBr die (Aldrich). Pellets were fired either in air or within a tube furnace under flowing oxygen for 12 h to several days at a chosen temperature between 600°C and 1100°C. Alumina boats (Alfa Aesar) were used to hold most samples; where melting occurred, platinum crucibles (Refining Systems, Inc.) were used to avoid contamination. The cooling rate was also varied, either by simply shutting off the furnace, utilizing a programmed rate, or quenching the crucible in air or water. Optimum syntheses for each phase are described in Section 3.

Slow cooling a stoichiometric melt containing 10% excess H_3BO_3 grew single crystals of most of the observed phases. When this did not result in the desired phase, borax ($Na_2B_4O_7 \cdot 10H_2O$, Aldrich) was used as a flux agent to reduce the fusion temperature. Samples were fired as powders in platinum crucibles by heating at 10°C/min to the desired temperature (typically 1050°C), held there for 10 h, then cooled at 2°C/h to 600°C after which the furnace was turned off.

2.2. Analysis

Fired samples were ground with an agate mortar and pestle and analyzed in Bragg–Brentano geometry with a Siemens D500 diffractometer equipped with a diffracted beam monochromator (CuKα radiation). Single crystal specimens were mounted with epoxy on glass fibers and analyzed at room temperature on a Siemens P4 diffractometer using graphite monochromated MoKα radiation ($\lambda = 0.71073$ Å). Unit-cell determinations were typically based on 25 centered reflections. Data were corrected for absorption using a face-indexed analytical method after measuring the crystal dimensions. The Bruker SHELXTL software package was used to solve the structures (using direct methods) and refine them with the full-matrix least-squares method using F_o^2 data. Details of the data collections and their results are listed in Table 1. Due to the high quality of the specimens, an extinction correction was included in the refinement which converged to a non-negligible value.

3. Results and discussion

Four different cobalt borate phases could be prepared by solid-state syntheses: $Co_3(BO_3)O_2$, $Co_3(BO_3)_2$, $Co_2(B_2O_5)$, and $Co(B_4O_7)$. In general, it was found that all Co precursors were useful in preparing the first three phases by firing stoichiometric mixtures at 950°C for 1 day. As expected, samples are more prone to contamination by unreacted material when either of the cobalt oxides is used. The carbonate was found to be the most favorable precursor, as it is already quite finely ground and less hygroscopic. Boric acid was preferred as the boron source as it grinds well in the ball mill (in contrast to hand grinding), and the texture of the powdered mixtures is much more amenable to pressing than ones made with B_2O_3. The latter gives gritty, hygroscopic mixtures that often bind the shaft of the die. Pressing was not found to be essential for good product purity, but it made handling the samples much more convenient. Metal borates also have the advantage that when excess boric acid is used, the unreacted boron oxide can be easily removed by washing in hot water

Table 1
Crystal data and refinement results for $Co(B_4O_7)$, $Co_4(BO_2)_6O$, and $Co_2(B_2O_5)$

Empirical formula	CoB_4O_7	$Co_4B_6O_{13}$	$Co_2B_2O_5$
Formula weight	214.17	508.58	219.48
Crystal system, space group	Orthorhombic, *Pbca*	Cubic, $I\bar{4}3m$	Triclinic, $P\bar{1}$
Unit-cell dimensions	$a = 8.1189(7)$ Å	$a = 7.4825(3)$ Å	$a = 3.1689(3)$ Å, $\alpha = 104.253(4)^\circ$
	$b = 8.621(1)$ Å		$b = 6.1530(5)$ Å, $\beta = 90.821(4)^\circ$
	$c = 13.737(1)$ Å		$c = 9.2734(7)$ Å, $\gamma = 92.098(5)^\circ$
Volume (Å^3)	961.5(2)	418.93(3)	175.08(3)
Z, calculated density (g/cm^3)	8, 2.959	2, 4.032	2, 4.163
Absorption coefficient (mm^{-1})	3.548	7.878	9.362
$F(000)$	824	484	208
Crystal color, habit	Purple plate	Dark violet dodecahedron	Purple needle prism
Crystal size (mm^3)	$0.30 \times 0.24 \times 0.08$	$0.16 \times 0.16 \times 0.16$	$0.21 \times 0.04 \times 0.04$
θ range for data collection (deg)	2.97–34.99	3.85–44.53	2.27 to 34.99
Limiting indices	$0 \leqslant h \leqslant 13$, $0 \leqslant k \leqslant 13$, $0 \leqslant l \leqslant 22$	$0 \leqslant h \leqslant 14$, $0 \leqslant k \leqslant 14$, $0 \leqslant l \leqslant 14$	$-5 \leqslant h \leqslant 5$, $-9 \leqslant k \leqslant 9$, $-14 \leqslant l \leqslant 14$
Reflections collected/unique	2115/2115 [$R_{int} = 0.0000$]	988/201 [$R_{int} = 0.0393$]	3041/1521 [$R_{int} = 0.0132$]
Completeness to θ_{max}	100.0%	100.0%	99.2%
Max. and min. transmission	0.754 and 0.460	0.409 and 0.370	0.734 and 0.639
Data/restraints/parameters	2115/0/110	201/0/14	1521/0/83
Goodness-of-fit on F^2	1.966	2.275	1.673
Final R indices [$I > 2\sigma(I)$]	$R_1 = 0.0319$, w$R_2 = 0.0693$	$R_1 = 0.0176$, w$R_2 = 0.0373$	$R_1 = 0.0159$, w$R_2 = 0.0366$
R indices (all data)	$R_1 = 0.0401$, w$R_2 = 0.0698$	$R_1 = 0.0176$, w$R_2 = 0.0373$	$R_1 = 0.0192$, w$R_2 = 0.0367$
Extinction coefficient	0.0145(4)	0.063(5)	0.0552(16)
Absolute structure parameter	—	−0.04(3)	—
Largest diff. peak and hole (e/Å^3)	0.969 and −0.896	0.569 and −0.744	0.543 and −0.720

Table 2
Atomic coordinates ($\times 10^4$), isotropic and anisotropic displacement parameters (Å$^2 \times 10^4$) for $Co(B_4O_7)$

Atom	x	y	z	U_{iso}	U_{11}	U_{22}	U_{33}	U_{23}	U_{13}	U_{12}
Co(1)	1108(1)	1189(1)	1180(1)	81(1)	88(1)	86(1)	68(1)	19(1)	14(1)	−13(1)
O(1)	988(2)	4379(2)	2007(1)	79(2)	103(6)	66(5)	69(5)	25(4)	21(5)	24(5)
O(2)	3510(2)	1611(2)	1068(1)	66(2)	73(5)	50(5)	73(6)	27(4)	−7(4)	−5(4)
O(3)	3193(2)	3919(2)	35(1)	97(3)	84(6)	86(6)	121(6)	43(5)	−39(5)	−19(5)
O(4)	4768(2)	4035(2)	1439(1)	84(3)	136(6)	58(6)	58(5)	5(4)	−20(5)	−5(5)
O(5)	5209(2)	1885(2)	2507(1)	96(3)	162(6)	58(5)	69(5)	5(5)	−45(5)	−12(5)
O(6)	5694(2)	2561(2)	42(1)	85(2)	97(6)	81(5)	78(5)	26(5)	37(5)	23(5)
O(7)	6227(2)	486(2)	1134(1)	118(3)	99(6)	137(6)	119(6)	64(5)	45(5)	42(5)
B(1)	4218(3)	2979(2)	631(2)	66(3)	80(8)	57(8)	61(7)	6(6)	−8(6)	−8(7)
B(2)	5315(3)	3456(2)	2312(2)	69(3)	73(8)	67(8)	67(8)	−3(6)	4(6)	5(6)
B(3)	4721(3)	783(2)	1664(2)	73(3)	83(8)	63(8)	74(8)	5(7)	−10(7)	−1(7)
B(4)	6701(3)	1367(2)	377(2)	79(3)	81(8)	90(9)	67(8)	3(7)	13(7)	6(7)

without destroying the target phase. Thus, for the highest purity $Co_3(BO_3)O_2$, $Co_3(BO_3)_2$, and $Co_2(B_2O_5)$, samples were prepared from stoichiometric mixtures of $CoCO_3$ and H_3BO_3; i.e., the extra hydrate mass in the carbonate salt was ignored, resulting in precursors that contained a slight excess of boric acid. After firing, the products were ground and stirred in hot water for 15 min, filtered and dried at 150°C.

For samples with a B:Co ratio of 5:1 or greater, a new phase was observed. Comparison of the diffraction pattern with that calculated for $Mn(B_4O_7)$ [25] indicated probable isomorphism, and this was confirmed by single crystal analysis (see below). This phase forms between 600°C and 890°C, above which it decomposes to the pyroborate and molten boron oxide. The pure form is best prepared by firing a mixture of 5 H_3BO_3: 1 $CoCO_3$ for 1 day at 880°C, then grinding, washing, and drying the product as above. Due to its thermal instability, however, single crystals of this compound cannot be grown from the melt.

By using flux methods, single crystals of $Co(B_4O_7)$ and two new phases were fortuitously prepared. A mixture of 10 H_3BO_3: 1 $CoCO_3$ was fired in air for 2 days at 800°C, ground and weighed. A mass of $Na_2B_4O_7 \cdot 10H_2O$

equal to one-half of the product mass was dehydrated overnight at 300°C, then mechanically ground with the product mixture and fired in a gold crucible. The temperature was raised 10°C/min to 800°C, held there for 10 h, then cooled at 2°C/h to 600°C after which the furnace was turned off. This yielded a mixture of parallel-grown bright purple plates of $Co(B_4O_7)$, pink fragments of $Na_2Co_2B_{12}O_{21}$ [7], colorless shards of unreacted flux, and a few tiny dark purple dodecahedra. Single crystal analysis of this last phase identified it as $Co_4(BO_2)_6O$, another new compound.

Many attempts were carried out to produce bulk quantities of $Co_4(BO_2)_6O$ by solid-state synthesis; however, none were successful. It is predicted that the conditions necessary to form this phase include higher pressure, just as for the Hg analogue [30]. The structure contains boron only in tetrahedral coordination, and research has shown that this is favored by increased pressure, yielding other interesting phases such as the zircon analogs [44,45], the fascinating new $Dy_4B_6O_{15}$ phase [47], and polymorphism in CaB_2O_4 [48]. As discussed below, the structure of this compound implies magnetic frustration [49] on the cobalt ion sites, and studies of its properties are highly desirable.

In summary, five phases in the Co–B–O system have been detected, four of them attainable by simple solid-state reaction. Only three of these are indicated on the original $CoO–B_2O_3$ phase diagram: $Co_3(BO_3)_2$, $Co_2(B_2O_5)$, and the additional phase which we have confirmed to be $Co(B_4O_7)$. Reaction of B_2O_3 with CoO (or any other Co source) also forms the $Co_3(BO_3)O_2$ phase, but requires temperatures greater than 800°C to improve purity. No phases were found with Co solely in the trivalent state, even when precursors (such as $Co(acac)_3$) were fired under pure oxygen, nor was there any detection of a mixed-valent warwickite phase. This preference for divalence mirrors the cobalt oxides, where Co_3O_4 decomposes to CoO with temperature and no strong evidence for Co_2O_3 has been provided [50].

3.1. Description of the structures

Initial searches of the Powder Diffraction File using product powder XRD patterns yielded poor matches, with the exception of samples containing $Co_3(BO_3)_2$. Consequently, we undertook a study of single crystal samples, both to identify the unknown phases and to refine some of the older structures. Where applicable, the labeling scheme from the original example of each framework has been used.

The tetraborate $Co(B_4O_7)$ exhibits the $Cd(B_4O_7)$ structure [27], also known for Mn [25], Zn [26], Hg [28], and Mg [51]. Atomic coordinates and anisotropic thermal parameters are listed in Table 2. The structure contains cobalt in highly distorted tetrahedral coordina-

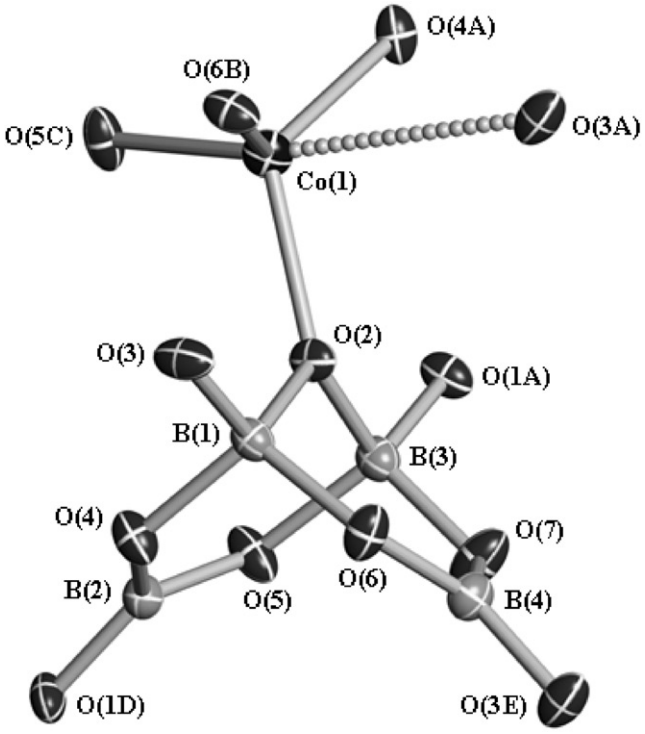

Fig. 1. Thermal ellipsoid plot of the cobalt and boron coordination environments within $Co(B_4O_7)$ at the 80% probability level. Symmetry labels correspond to those defined in Table 3.

Table 3
Bond lengths (Å) and angles (deg) for $Co(B_4O_7)$

Cobalt coordination			
Co(1)–O(2)	1.990(1)	O(2)–Co(1)–O(4A)	121.78(6)
Co(1)–O(4A)	2.020(1)	O(2)–Co(1)–O(6B)	90.07(6)
Co(1)–O(6B)	2.023(1)	O(4A)–Co(1)–O(6B)	125.29(6)
Co(1)–O(5C)	2.036(1)	O(2)–Co(1)–O(5C)	111.45(6)
Co(1)–O(3A)	2.574(2)	O(4A)–Co(1)–O(5C)	89.34(6)
		O(6B)–Co(1)–O(5C)	121.23(6)
Boron coordination			
B(1)–O(2)	1.442(2)	O(3)–B(1)–O(2)	118.2(2)
B(1)–O(3)	1.422(2)	O(3)–B(1)–O(6)	107.2(2)
B(1)–O(4)	1.504(2)	O(2)–B(1)–O(6)	110.4(2)
B(1)–O(6)	1.489(2)	O(3)–B(1)–O(4)	104.7(2)
B(2)–O(1D)	1.344(2)	O(2)–B(1)–O(4)	107.9(2)
B(2)–O(4)	1.373(2)	O(6)–B(1)–O(4)	108.0(2)
B(2)–O(5)	1.383(2)	O(1D)–B(2)–O(4)	121.6(2)
B(3)–O(1A)	1.421(3)	O(1D)–B(2)–O(5)	118.0(2)
B(3)–O(2)	1.465(2)	O(4)–B(2)–O(5)	120.4(2)
B(3)–O(5)	1.549(3)	O(1A)–B(3)–O(7)	111.0(2)
B(3)–O(7)	1.446(3)	O(1A)–B(3)–O(2)	109.4(2)
B(4)–O(3E)	1.359(3)	O(7)–B(3)–O(2)	111.8(2)
B(4)–O(6)	1.392(3)	O(1A)–B(3)–O(5)	112.2(2)
B(4)–O(7)	1.343(2)	O(7)–B(3)–O(5)	105.6(2)
		O(2)–B(3)–O(5)	106.9(2)
		O(7)–B(4)–O(3E)	118.3(2)
		O(7)–B(4)–O(6)	120.3(2)
		O(3E)–B(4)–O(6)	121.3(2)

Symmetry transformations used to generate equivalent atoms: A: $-x+1/2, y-1/2, z$; B: $x-1/2, -y+1/2, -z$; C: $x-1/2, y, -z+1/2$; E: $x+1/2, y, -z+1/2$; F: $x+1/2, -y+1/2, -z$.

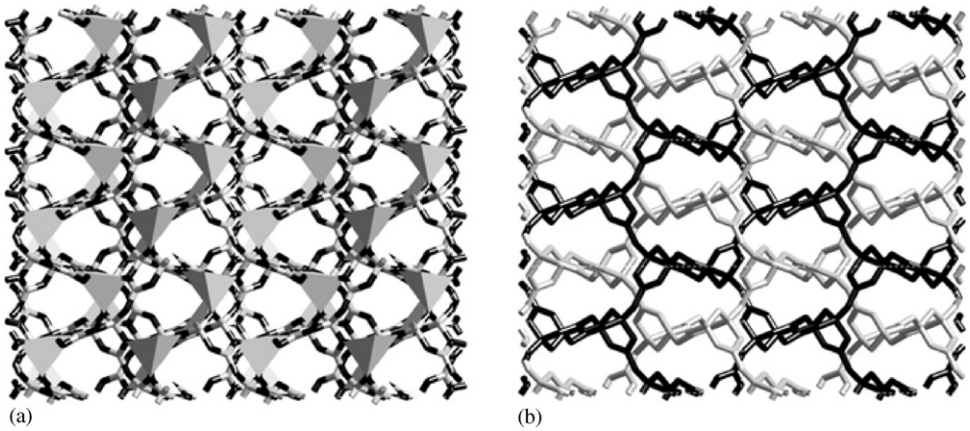

Fig. 2. (a) View along [010] of the connectivity within $Co(B_4O_7)$, with cobalt sites shown as distorted tetrahedra, boron, and oxygen atoms shown as light and dark cylinders, respectively. (b) The same view, with the omission of the cobalt ions, illustrating the two interpenetrated tetraborate networks.

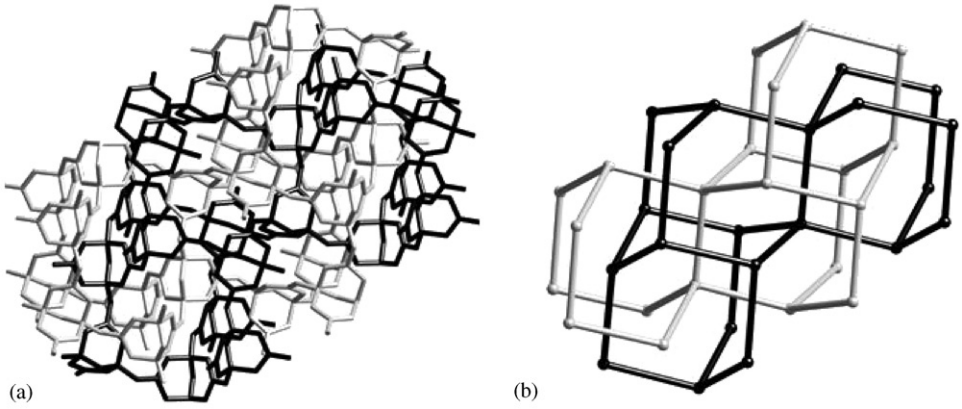

Fig. 3. The two interpenetrated networks in $Co(B_4O_7)$, shaded light and dark in (a), have been deconstructed as identical cubic diamond topologies in (b) by drawing connections between the centers of each tetraborate building unit.

Table 4
Atomic coordinates ($\times 10^5$), isotropic and anisotropic displacement parameters ($Å^2 \times 10^4$) for $Co_4(BO_2)_6O$

Atom	x	y	z	U_{iso}	U_{11}	U_{22}	U_{33}	U_{23}	U_{13}	U_{12}
Co(1)	15 340(3)	15 340(3)	15 340(3)	51.8(8)	51.8(8)	51.8(8)	51.8(8)	–4.1(6)	–4.1(6)	–4.1(6)
O(1)	0	0	0	55(5)	55(5)	55(5)	55(5)	0	0	0
O(2)	14 067(11)	14 067(11)	41 641(14)	49(1)	55(2)	55(2)	37(3)	54(2)	54(2)	21(3)
B(1)	25 000	50 000	0	48(3)	52(6)	46(4)	46(4)	0	0	0

tion, with an additional long contact by O(3) at 2.57 Å (see Fig. 1 and Table 3). This coordination explains the vivid purple color of the compound, as $d \rightarrow d$ electronic transitions are Laporte allowed. The isolated coordination sites of cobalt link two interpenetrated metaborate networks, as shown in Fig. 2. This interpenetration was noted in the original $Cd(B_4O_7)$ structural analysis, and several other examples exist [52]. In addition, it is instructive to note the basic symmetry buried within the structure: each net is formed by the condensation of approximately tetrahedral B_4O_9 units, giving rise to the cubic diamond topology illustrated in Fig. 3.

The metaborate oxide $Co_4(BO_2)_6O$ is the most intriguing compound in these findings, despite its low yield. It is isostructural with the Zn compound [29] and there is evidence for a Hg analogue formed under high-pressure [30], and chalcogenide-containing compounds [53,54]. Atomic coordinates and anisotropic thermal parameters are listed in Table 4. The structure consists of μ^4-oxo centered cobalt tetrahedra housed within

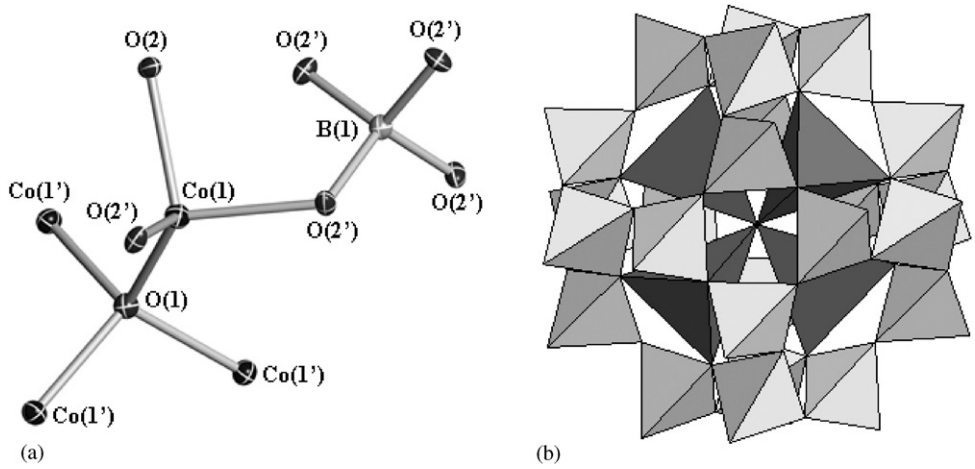

Fig. 4. (a) Thermal ellipsoid plot of the cobalt and boron coordination environments within $Co_4(BO_2)_6O$ at the 80% probability level, with primes indicating symmetry generated atoms. (b) Polyhedral view of the metaborate cage within $Co_4(BO_2)_6O$, housing the Co_4O units. Cobalt and boron coordinations are shown as dark and light tetrahedra, respectively.

Table 5
Bond lengths (Å) and angles (deg) for $Co_4(BO_2)_6O$

Cobalt coordination			
Co(1)–O(1)	1.9881(4)	O(1)–Co(1)–O(2)	121.35(4)
Co(1)–O(2)	1.9726(10)	O(2)–Co(1)–O(2A)	95.40(5)
Boron coordination			
B(1)–O(2A)	1.4725(4)	O(2A)–B(1)–O(2B)	107.98(4)
		O(2A)–B(1)–O(2C)	112.50(8)

Symmetry transformations used to generate equivalent atoms: A: y, z, x; B: $-x+1/2, y+1/2, -z+1/2$; C: $y, -z+1, -x$.

cages of an infinite metaborate framework (see Fig. 4 and Table 5). Boron is found in tetrahedral coordination yielding a sodalite topology; consequently, this network has inspired researchers searching for borate open frameworks [38,55]. The structure is clearly quite dense, but it is the isolation of the Co_4O units that interests us. This tetrahedral array predicts interesting magnetic behavior, as superexchange between adjacent atoms cannot satisfy antiparallel coupling for all of them. This behavior has been studied for a number of compounds where the interaction extends across the entire lattice, including the "spin ice" pyrochlores [49,56], but it is unknown how these isolated frustrated clusters would behave. Clearly, study of these properties begs the development of a high yield synthesis for this compound.

The pyroborate $Co_2(B_2O_5)$ has been known for some time [11], and the present structure determination refines the crystallographic parameters and bond lengths of this compound. In doing so, we have generated a structure (see Tables 6 and 7) for which the calculated powder XRD pattern exactly matches that of the solid-state reaction product. In addition, the bond lengths within the pyroborate unit, shown in Fig. 5, have been accurately determined and illustrate the asymmetry in bonding between the terminal and bridging oxygens. The two BO_3 triangles are essentially planar, and are 16° out of planarity with each other. They serve to bridge the 4×1 sheets of edge-shared CoO_6 octahedra by both corner- and edge-sharing as illustrated in Fig. 6. The magnesium [57] and cadmium [39] analogues of this compound have been established, although the latter is most likely in the incorrect space group.

The orthoborate, $Co_3(BO_3)_2$, and ludwigite, $Co_3(BO_3)O_2$ structures have been refined recently [13,14] and are mentioned here for completeness. Both contain edge- and corner-shared octahedral metal sites surrounding isolated, parallel borate triangles, as illustrated in Figs. 7 and 8. The magnetic behavior of the orthoborate has been studied; the compound is antiferromagnetic below 37 K and neutron diffraction studies indexed the magnetic unit cell as a $a \times 2b \times 2c$ supercell [58]. Some magnetic measurements have been made on the cobalt ludwigite, but this has not been studied as exhaustively as the iron analogue [4].

4. Conclusions

The Co–B–O system has proven to be more structurally diverse than once thought. Its properties follow the trend along the first transition series, as cobalt prefers a divalent state in most of its compounds. In total, five crystalline ternary phases have been observed: $Co_3(BO_3)O_2$, $Co_3(BO_3)_2$, $Co_2(B_2O_5)$, $Co(B_4O_7)$, and the new phase $Co_4(BO_2)_6O$. The only phase that can be prepared by a solid-state route that contains cobalt in a higher oxidation state is the mixed-valent ludwigite,

Table 6
Atomic coordinates ($\times 10^4$), isotropic and anisotropic displacement parameters ($Å^2 \times 10^4$) for $Co_2(B_2O_5)$

Atom	x	y	z	U_{iso}	U_{11}	U_{22}	U_{33}	U_{23}	U_{13}	U_{12}
Co(1)	7299(1)	2124(1)	3590(1)	65.1(5)	71.4(9)	61.3(9)	59.9(9)	10.8(6)	−9.7(6)	1.1(6)
Co(2)	2345(1)	3716(1)	1017(1)	55.7(5)	62.7(9)	53.3(9)	51.1(9)	12.9(6)	−4.9(6)	4.0(6)
O(1)	2600(3)	6951(2)	538(1)	68(2)	86(4)	57(4)	53(4)	1(3)	−4(3)	6(3)
O(2)	2178(3)	922(2)	1808(1)	84(2)	125(5)	50(4)	78(4)	18(3)	−3(3)	13(3)
O(3)	7376(3)	4761(2)	2584(1)	69(2)	89(4)	51(4)	60(4)	−1(3)	−3(3)	13(3)
O(4)	5593(3)	8599(2)	2984(1)	88(2)	135(5)	53(4)	69(4)	5(3)	−38(3)	9(3)
O(5)	7721(3)	7244(2)	5027(1)	86(2)	85(4)	121(5)	47(4)	12(3)	−11(3)	13(3)
B(1)	6983(5)	6811(3)	3553(2)	62(2)	65(6)	61(6)	56(6)	8(5)	−7(4)	−3(5)
B(2)	3334(5)	8798(3)	1692(2)	64(2)	68(6)	63(6)	58(6)	8(5)	7(4)	−1(5)

Table 7
Bond lengths (Å) and angles (deg) for $Co_2(B_2O_5)$

Cobalt coordination			
Co(1)–O(5A)	1.985(1)	O(2)–Co(1)–O(2D)	88.22(4)
Co(1)–O(5B)	2.046(1)	O(3)–Co(1)–O(2)	79.31(4)
Co(1)–O(3)	2.061(1)	O(3)–Co(1)–O(2D)	80.24(4)
Co(1)–O(4C)	2.149(1)	O(4C)–Co(1)–O(2)	62.43(4)
Co(1)–O(2)	2.268(1)	O(4C)–Co(1)–O(2D)	80.40(4)
Co(1)–O(2D)	2.285(1)	O(5A)–Co(1)–O(2)	170.82(4)
Co(2)–O(2)	2.028(1)	O(5B)–Co(1)–O(2)	83.33(4)
Co(2)–O(1E)	2.074(1)	O(5B)–Co(1)–O(2D)	170.13(4)
Co(2)–O(3)	2.113(1)	O(5A)–Co(1)–O(2D)	84.25(4)
Co(2)–O(1)	2.143(1)	O(3)–Co(1)–O(4C)	137.32(4)
Co(2)–O(1F)	2.154(1)	O(5A)–Co(1)–O(3)	104.49(4)
Co(2)–O(3G)	2.164(1)	O(5B)–Co(1)–O(3)	103.08(4)
		O(5A)–Co(1)–O(4C)	110.93(4)
		O(5B)–Co(1)–O(4C)	91.14(4)
		O(5A)–Co(1)–O(5B)	103.65(5)
		O(1E)–Co(2)–O(1)	83.97(4)
		O(1)–Co(2)–O(1F)	83.63(4)
		O(1E)–Co(2)–O(1F)	97.11(4)
		O(2)–Co(2)–O(1)	171.07(4)
		O(2)–Co(2)–O(1E)	102.22(4)
		O(2)–Co(2)–O(1F)	101.77(4)
		O(3)–Co(2)–O(1)	89.85(4)
		O(1E)–Co(2)–O(3)	173.77(4)
		O(3)–Co(2)–O(1F)	82.98(4)
		O(1)–Co(2)–O(3G)	90.41(4)
		O(1E)–Co(2)–O(3G)	83.65(4)
		O(1F)–Co(2)–O(3G)	173.87(4)
		O(2)–Co(2)–O(3)	83.83(4)
		O(2)–Co(2)–O(3G)	83.96(4)
		O(3)–Co(2)–O(3G)	95.61(4)
Boron coordination			
B(1)–O(3)	1.367(2)	O(3)–B(1)–O(4)	118.4(1)
B(1)–O(4)	1.413(2)	O(3)–B(1)–O(5)	124.6(1)
B(1)–O(5)	1.342(2)	O(4)–B(1)–O(5)	117.0(1)
B(2)–O(1)	1.366(2)	O(1)–B(2)–O(2H)	128.6(1)
B(2)–O(2H)	1.350(2)	O(1)–B(2)–O(4)	119.8(1)
B(2)–O(4)	1.420(2)	O(2H)–B(2)–O(4)	111.6(1)
		B(1)–O(4)–B(2)	135.8(1)

Symmetry transformations used to generate equivalent atoms: A: $-x+2,-y+1,-z+1$; B: $-x+1,-y+1,-z+1$; C: $x,y-1,z$; D:$x+1,y,z$; E: $-x,-y+1,-z$; F: $-x+1,-y+1,-z$; G: $x-1,y,z$; H: $x,y+1,z$.

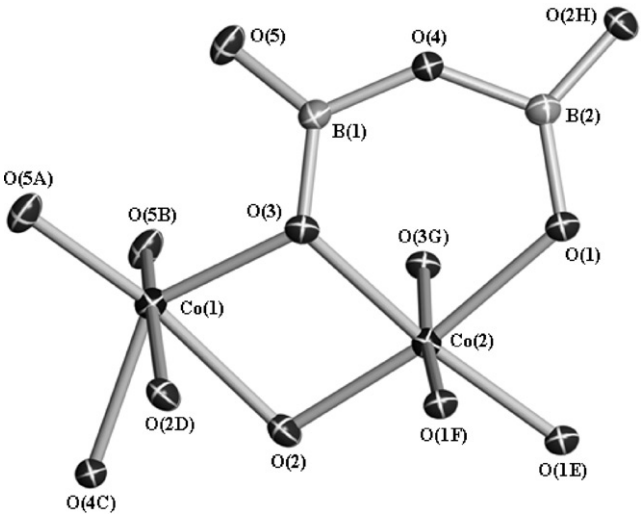

Fig. 5. Thermal ellipsoid plot of the cobalt and boron coordination environments within $Co_2(B_2O_5)$ at the 80% probability level. Symmetry labels correspond to those defined in Table 7.

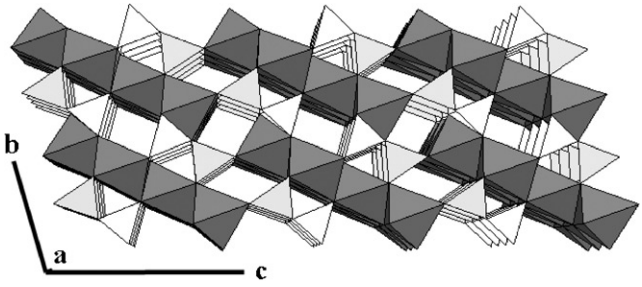

Fig. 6. View along [100] of the connectivity within $Co_2(B_2O_5)$, with cobalt sites shown as dark octahedra, and boron as light triangles. The pyroborate units pin together the 4×1 octahedral ribbons by both edge and corner sharing.

even when starting materials are fired under a pure oxygen atmosphere. The $Co_4(BO_2)_6O$ compound warrants magnetic studies as it is predicted to show frustrated behavior. Attempts at preparing this compound by alternate routes are currently underway.

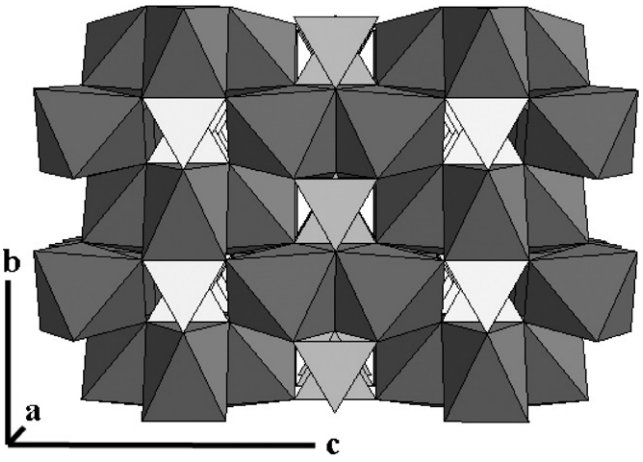

Fig. 7. View along [100] of the connectivity within $Co_3(BO_3)_2$, with cobalt sites shown as dark octahedra, and boron as light triangles. The borate units are housed between rows of edge-shared cobalt octahedra, which are in turn connected to each other by corner sharing.

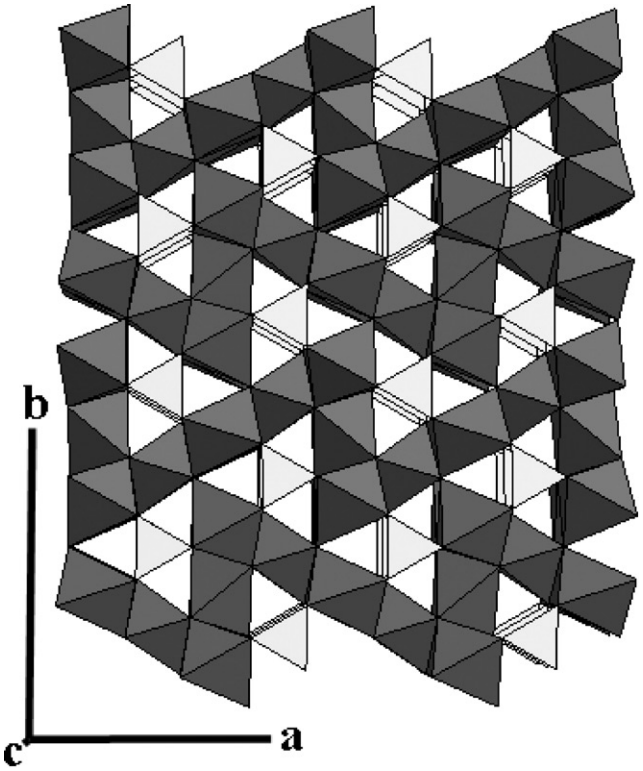

Fig. 8. View along [001] of the connectivity within $Co_3(BO_3)O_2$, with cobalt sites shown as dark octahedra, and boron as light triangles. The borate units are housed between zig-zag walls of edge-shared cobalt octahedra, which are connected by corner sharing.

Acknowledgments

We thank the NSERC (Canada) for financial support through their Research, Strategic, and Scholarship programs.

References

[1] P. Becker, Adv. Mater. 10 (1998) 979;
D.A. Keszler, Curr. Opin. Solid State Mater. Sci. 4 (1999) 155;
T. Sasaki, Y. Mori, M. Yoshimura, Y.K. Yap, T. Kamimura, Mater. Sci. Eng. R. 30 (2000) 1.
[2] A. Zletz (Amoco Corp.), US Patent Application 709, 790, 11 March 1985.
[3] J.P. Attfield, A.M.T. Bell, L.M. Rodriguez-Martinez, J.M. Greneche, R. Retoux, M. Leblanc, R.J. Cernik, J.F. Clarke, D.A. Perkins, J. Mater. Chem. 9 (1999) 205.
[4] R. Wolfe, R.D. Pierce, M. Eibschut, J.W. Nielsen, Solid State Commun. 7 (1969) 949;
R.B. Guimaraes, M. Mir, J.C. Fernandes, M.A. Continentino, H.A. Borges, G. Cernicchiaro, M.B. Fontes, D.R.S. Candela, E. Baggio-Saitovitch, Phys. Rev. B 60 (1999) 6617;
N.B. Ivanova, V.V. Rudenko, A.D. Balaev, N.V. Kazak, V.V. Markov, S.G. Ovchinnikov, I.S. Edel'man, A.S. Fedorov, P.V. Avramov, J. Exp. Theoret. Phys. 94 (2002) 299.
[5] V. Legagneur, Y. An, A. Mosbah, R. Portal, A. Le Gal La Salle, A. Verbaere, D. Guyomard, Y. Piffard, Solid State Ionics 139 (2001) 37;
A. Ibarra-Palos, C. Darie, O. Proux, J.L. Hazemann, L. Aldon, J.C. Jumas, M. Morcrette, P. Strobel, Chem. Mater. 14 (2002) 1166.
[6] J.L.C. Rowsell, L.F. Nazar, J. Mater. Chem. 11 (2001) 3228.
[7] J.L.C. Rowsell, N.J. Taylor, L.F. Nazar, J. Am. Chem. Soc. 124 (2002) 6522.
[8] P.F. Konovalov, Dokl. Akad. Nauk SSSR 70 (1950) 847;
I.N. Belyaev, Zh. Fiz. Khim. 30 (1956) 1419.
[9] D. Hauck, F. Muller, Z. Anorg. Allg. Chem. 466 (1980) 163.
[10] S.V. Berger, Acta Chem. Scand. 3 (1949) 660.
[11] S.V. Berger, Acta Chem. Scand. 4 (1950) 1054.
[12] W. Gotz, V. Hermann, Naturwissenschaften 53 (1966) 475.
[13] H. Effenberger, F. Pertlik, Z. Kristallogr. 166 (1984) 129.
[14] R. Norrestam, K. Nielsen, I. Sotofte, N. Thorup, Z. Kristallogr. 189 (1989) 33.
[15] D.A. Keszler, H. Sun, Acta Crystallogr. C 44 (1988) 1505.
[16] M. Huber, H.J. Deiseroth, Z. Kristallogr. NCS 210 (1995) 685.
[17] H. Schmid, Acta Crystallogr. 17 (1964) 1080.
[18] N.C. Tombs, W.J. Croft, H.C. Mattraw, Inorg. Chem. 2 (1963) 872.
[19] R. Diehl, Solid State Commun. 17 (1975) 743.
[20] R. Diehl, G. Brandt, Acta Crystallogr. B 31 (1975) 1662.
[21] A. Utzolino, K. Bluhm, Z. Naturforsch. 51b (1996) 1433.
[22] J.S. Swinnea, H. Steinfink, Am. Mineral. 5 (1983) 827.
[23] R. Norrestam, M. Kritikos, A. Sjodin, J. Solid State Chem. 114 (1995) 311.
[24] L.V. Lavriv, V.N. Pavlikov, E.S. Lugovskaya, Ukrain. Khim. Zh. 56 (1990) 455.
[25] S.C. Abrahams, J.L. Bernstein, P. Gibart, M. Robbins, R.C. Sherwood, J. Chem. Phys. 60 (1974) 1899.
[26] M. Martinez-Ripoll, S. Martinez-Carrera, S. Garcia-Blanco, Acta Crystallogr. B 27 (1971) 672.
[27] M. Ihara, J. Krogh-Moe, Acta Crystallogr. 20 (1966) 132.
[28] Y. Laureiro, M.L. Veiga, A. Jerez, C. Pico, Polyhedron 8 (1989) 1567.
[29] P. Smith-Verdier, S. Garcia-Blanco, Z. Kristallogr. 151 (1980) 175.
[30] C.H. Chang, J.L. Margrave, Inorg. Chim. Acta 1 (1967) 378.
[31] M. Martinez-Ripoll, S. Martinez-Carrera, S. Garcia-Blanco, Acta Crystallogr. B 27 (1971) 677.
[32] W. Depmeier, H. Schmid, Acta Crystallogr. B 38 (1982) 605.
[33] H. Behm, Acta Crystallogr. B 38 (1982) 2781.
[34] W.H. Baur, E. Tillmanns, Z. Kristallogr. 131 (1970) 213.

[35] Y. Laureiro, M.L. Veiga, J. Isasi, E. Ramos, A. Jerez, C. Pico, J. Mater. Sci. Lett. 10 (1991) 635.
[36] O.S. Bondareva, M.A. Simonov, N.V. Belov, Sov. Phys. Crystallogr. 23 (1978) 272.
[37] Y. Laureiro, M.L. Veiga, M.L. Lopez, S. Garcia-Martin, A. Jerez, C. Pico, Powder Diff. 6 (1991) 28.
[38] W.T.A. Harrison, T.E. Gier, G.D. Stucky, Angew. Chem. Int. Ed. Engl. 32 (1993) 724.
[39] E.V. Sokolova, M.A. Simonov, N.V. Belov, Sov. Phys. Dokl. 24 (1979) 524.
[40] G. Brachtel, M. Jansen, Z. Anorg. Allg. Chem. 478 (1981) 13.
[41] J. Krogh-Moe, Acta Crystallogr. 18 (1965) 77.
[42] M. Jansen, W. Scheld, Z. Anorg. Allg. Chem. 477 (1981) 85.
[43] M. Jansen, G. Brachtel, Z. Anorg. Allg. Chem. 489 (1982) 42.
[44] K-J. Range, M. Wildenauer, A.M. Heyns, Angew. Chem. Int. Ed. Engl. 27 (1988) 969.
[45] K-J. Range, M. Wildenauer, M. Andratschke, Z. Kristallogr. 211 (1996) 815.
[46] C.L. Christ, J.R. Clark, Phys. Chem. Minerals 2 (1977) 59; P.C. Burns, J.D. Grice, F.C. Hawthorne, Can. Mineral. 33 (1995) 1131.
[47] H. Huppertz, B. von der Eltz, J. Amer. Chem. Soc. 124 (2002) 9376.
[48] M. Marezio, J.P. Remeika, P.D. Dernier, Acta Crystallogr. B 25 (1969) 965.
[49] J.E. Greedan, J. Mater. Chem. 11 (2001) 37.
[50] N.N. Greenwood, A. Earnshaw, Chemistry of the Elements, 2nd Edition, Butterworth-Heinemann, Oxford, Boston, 1998, pp. 1117–1118.
[51] H. Bartl, W. Schuckmann, Neues Jahrb. Mineral. Monatsh. (1966) 142.
[52] J. Krogh-Moe, Acta Crystallogr. B 30 (1974) 747.
[53] C. Fouassier, A. Levasseur, J.C. Joubert, J. Muller, P. Hagenmuller, Z. Anorg. Allg. Chem. 375 (1970) 202.
[54] A. Levasseur, B. Rouby, C. Fouassier, C. R. Acad. Sci. Paris Ser. C 277 (1973) 421.
[55] A. Choudhury, S. Neeraj, S. Natarajan, C.N.R. Rao, Dalton Trans. 7 (2002) 1535.
[56] S.T. Bramwell, M.J.P. Gingras, Science 294 (2001) 1495.
[57] G.C. Guo, W.D. Cheng, J.T. Chen, J.S. Huang, Q.E. Zhang, Acta Crystallogr. C 51 (1995) 351.
[58] R.E. Newnham, M.J. Redman, R.P. Santoro, Z. Kristallogr. 121 (1965) 418.